

Research Article

Adaptive Teleoperation System with Neural Network-Based Multiple Model Control

Vu Trieu Minh and Fakhruddin Mohd Hashim

Mechanical Engineering Department, Universiti Teknologi Petronas (UTP), Bandar Seri Iskandar, 31750 Tronoh, Perak, Malaysia

Correspondence should be addressed to Vu Trieu Minh, vutrieuminh@yahoo.com

Received 31 March 2010; Revised 19 July 2010; Accepted 22 July 2010

Academic Editor: Massimo Scalia

Copyright © 2010 V. T. Minh and F. Mohd Hashim. This is an open access article distributed under the Creative Commons Attribution License, which permits unrestricted use, distribution, and reproduction in any medium, provided the original work is properly cited.

This paper presents an adaptive teleoperation which is robust to time-delay and environmental uncertainties while assuring the transparent performance. A novel theoretical framework and algorithms for the teleoperation system have been built up with neural network-based multiple model control and time forward state observer. Conditions for stability and transparency performance are also identified. Simulations show that the system is stable and in good performance.

1. Introduction

Applications of master-slave teleoperation system can be found in many areas from micro to macro scales. A teleoperation system or a bilateral telemanipulation system is a complex electro-mechanical system with a master and a slave device, interconnected by a communication channel and controller. Through interaction with the master device, the human operator is able to communicate control signals for the slave. The slave device actually interacts with the remote environments, thereby staying under full control of the human operator. Information gathered at the remote environments is transmitted back to the human operator through the master device. Usually a camera is installed at the slave device to provide the visual information to the operator.

The existence of varying time delays in the communication channel and the uncertainty of the remote environments are the most important problems regarding the stability of the teleoperation systems since they will cause bad performance or instability to the system. Another important aspect is the transparency or the transparent performance of the systems. The transparency is defined as the impedance felt by the human operator on the local site. This allows the operator to feel the real sense of the remote environments. It can be applied in the case, for example, where the medical doctors cannot approach the patients directly.

Delays in the communication channel make the standard control law nonpassive system. But by mimicking the lossless transmission line, the system becomes passive and, hence, stable. Kikuchi et al. [1] proposed a teleoperation system in dynamic environment with varying communication time delays. The proposed system consists of the stable bilateral teleoperation subsystem that offers pictures in remote site and the environment prediction display subsystem that offers the prediction of the slave manipulator and the environment. Zhu and Salcudean [2] introduced a novel stability guaranteed controller design for bilateral teleoperation under both position and rate control modes with arbitrary motion/force scaling. Boukhniifer and Ferreira [3] presented a bilateral controller for a micro-teleoperation system using passivity approaches. They showed that the application of wave variable formation allows the passivity of the system in spite of the communication delays and the varying scaling factors.

Transparency and stability in bilateral teleoperation systems have also been analyzed when communication delays are present. Lawrence [4] explored the trade-off algorithm between transparency and stability based on the concept of impedance, a quantity that maps the input position of a system to the output force. When a teleoperation system is ideal, the operator feels as if he is operating directly the remote environments. Slawiński and Mut [5] proposed defining transparency in the time domain and established a quantitative measure of how the human operator feels the remote system. It allows analyzing the effect of the time-varying delays on the system transparency.

The complexity of the uncertain remote environments makes the development of such exact models for all potential environments impossible. For the model detection, various methods have been developed. One of the most effective approaches is the use of multiple-model neural network. By very fast calculation, the neural network can select the most reliable model and provide the online optimal control action for the system. Most of the current employed neural networks for artificial intelligence are based on statistical estimation, optimization, and control theory. Chen et al. [6] proposed a neural network-based multiple-model adaptive control for teleoperation system. Decision controller is designed to adaptive switch among all predictive controllers according to the performance target. This method can ensure the stability and transparent performance of the system. Smith and Hashtrudi-Zaad [7] used two neural networks at the master and slave devices to improve the transparency and to compensate the effect of the time delays.

This paper presents a novel scheme to control the displacement and force for a bilateral teleoperation system in variant time delays and environmental uncertainties. The aim of the paper is to develop a simple and low cost teleoperation connected via the global internet system (Internet Protocol Suite—TCP/IP) and without a camera in the slave device. The system can be supported by a telephone or voice chat over Internet Protocol (VoIP) for a medical doctor who can use the hands/fingers to examine the remote patients. The idea of the system is initiated from the design of a medical teleanalyzer in Suebsomran and Parnichkun [8] who introduced a hybrid teleoperation controller of displacement and force, which is robust to internal and external disturbances, model uncertainty, load, and friction. The teleoperation transparency in time delays and the effect of local force feedback were also investigated by Hashtrudi-Zaad and Salcudean [9] where the stability robustness of the system was analyzed and the transparency conditions for a general teleoperation system are presented. The environment uncertainty modeling and verification are referred to by Minh V.T et al. in [10]. The stability of uncertain cellular neural networks and the stability criterion for bidirectional associative memory neural networks with interval time-varying delays are also referred to by Kwon and Park in [11, 12].

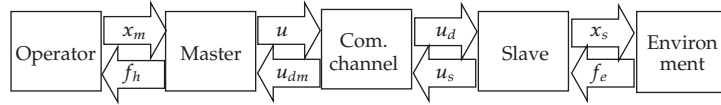


Figure 1: Teleoperation system configuration.

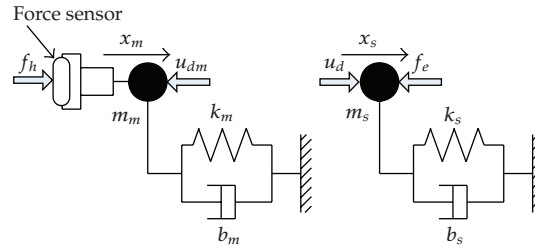


Figure 2: Physical model of master and slave manipulator.

The followings are the content of this paper: Section 2 introduces the system modeling; Section 3 develops the system time forward observer; Section 4 sets up stability and transparency conditions for the system controller; Section 5 illustrates simulation results; and finally conclusions are drawn in Section 6.

2. System Modeling

As mentioned in the introduction part, a teleoperation system consists of four fundamental components: the human operator, the communication channel, the slave manipulator, and the environment. Through these five components, information is exchanged in two directions. The control channel enables the human operator to assign tasks to the slave and control the slave as desired. Then, information about the task execution is fed back to the human operator. Both channels are interconnected via the normal internet system. For the simplification and low cost purpose, there is no camera installed in the slave device—a voice chat over Internet Protocol can support the communication between the doctor and the patient instead. Figure 1 shows the basic configuration for a bilateral control setting adopted by the position-force controller architecture by Lawrence [4]: the operator moves the master manipulator and via the Internet channel communication, the slave manipulator follows. Forces exerted by the environment on the slave are transmitted back to the master and felt by the operator.

The human force on the master f_h and the master motion x_m should have the same relationship with the force on the environment f_e and the slave motion x_s , that is, for the same forces, $f_e = f_h$, the motions should be the same, $x_s = x_m$. This requirement assures that the system is completely transparent. So the operator feels the real sense of the remote environments. Notations, u , u_{dm} , u_d , and u_s , are the signals transmitted among the system's components.

The master and slave are all modeled as mechanical devices with masses, dampers, and springs, as shown in Figure 2.

The human force f_h is applied to the master manipulator and x_m is the position of the master; f_e is the contact force between the slave manipulator and the environment, and x_s

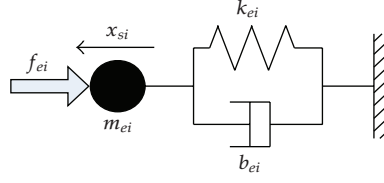


Figure 3: Physical Model of Environment.

is the position of the slave; u_{dm} is the feedback signal from the slave, and u_d is the control signal given by the master through the Internet. Notations, m_m , m_s , b_m , b_s , k_m , and k_s , are the inertia, damping, and spring stiffness of the master and slave manipulator, respectively.

The dynamics of the master and the slave are given by the following equations:

$$f_h - u_{dm} = m_m \ddot{x}_m + b_m \dot{x}_m + k_m x_m, \quad (2.1)$$

$$u_d - f_e = m_s \ddot{x}_s + b_s \dot{x}_s + k_s x_s. \quad (2.2)$$

For the variant time delays and the environmental uncertainties, it is assumed that the dynamics of the environment are also regulated by a finite set of mechanical devices with masses, dampers, and springs, shown in Figure 3: x_{si} denotes the position of the slave device and f_{ei} denotes the force applied on the environment i . Similarly, m_{ei} , k_{ei} , and b_{ei} are mass, stiffness and damping parameters of the unknown and time-variant environment models.

The dynamics of the environment model are formulated by the following equation:

$$f_e = m_e \ddot{x}_s + b_e \dot{x}_s + k_e x_s \quad \text{or} \quad f_{ei} = m_{ei} \ddot{x}_{si} + b_{ei} \dot{x}_{si} + k_{ei} x_{si}, \quad \text{for } i = 1, \dots, n. \quad (2.3)$$

Since the environment models are uncertain, a neural network with the radial basis function (RBF) is used to detect the environmental dynamics since RBF network is easy to approximate the parameters and the training speed is fast. For n given environment models, the input vectors U is the movement of the slave device

$$U = \begin{bmatrix} x_{s1} & \cdots & x_{sn} \\ \dot{x}_{s1} & \cdots & \dot{x}_{sn} \\ \ddot{x}_{s1} & \cdots & \ddot{x}_{sn} \end{bmatrix}, \quad (2.4)$$

and the target vectors Y is the environment model parameters:

$$Y = \begin{bmatrix} k_{e1} & \cdots & k_{en} \\ b_{e1} & \cdots & b_{en} \\ m_{e1} & \cdots & m_{en} \end{bmatrix}. \quad (2.5)$$

From the online archived slave movements, $[x_{si} \ \dot{x}_{si} \ \ddot{x}_{si}]'$, RBF will on line calculate the corresponding environment parameters, $[\hat{k}_{ei} \ \hat{b}_{ei} \ \hat{m}_{ei}]'$, and, then, the corresponding model errors $\epsilon_i = \sqrt{[m_{ei} - \hat{m}_{ei}]^2 + [b_{ei} - \hat{b}_{ei}]^2 + [k_{ei} - \hat{k}_{ei}]^2}$. If the ϵ_m is the smallest, the m th

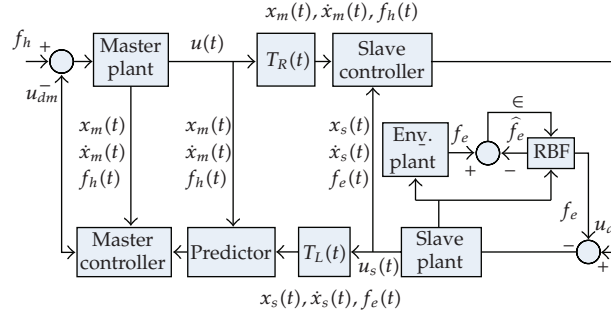


Figure 4: Schematic Diagram of the Teleoperation System.

environment model which fits the best to the current dynamics is selected. The environment modeling and verification are referred to by Minh. et al. in [10]. It is assumed that the environmental uncertainties can be represented by mathematical models. To each model, the system behavior changes and should be estimated by a different modes. The system mode may jump up or vary continuously in a discrete set.

Since the master and the slave devices are connected via the Internet, the time delay is significant and variant. Thus, the equations for signal transmitted via communication channel must include the forward time delay, $T_R(t)$, and the backward time delay, $T_L(t)$:

$$\begin{aligned} u_d &= u(t - T_R(t)), \\ u_{dm} &= u_s(t - T_L(t)). \end{aligned} \quad (2.6)$$

Finally the overall schematic diagram of the proposed system is show in Figure 4.

The operator moves the master plant, which causes a transmitted signal, $u(t)$. In conventional methods proposed by Lawrence [4] and Hashtrudi-Zaad and Salcudean [9], the transmitted signals include position, velocity, and acceleration. But in this proposed system, the operator (medical doctor) wants to directly and gently touch the patient, and the acceleration is difficult to be realized and can be omitted from the dynamic equations in order to guarantee the high transparency for the operator. Thus,

$$u(t) = f_{11}x_m(t) + f_{12}\dot{x}_m(t) + c_{11}f_h(t), \quad (2.7)$$

where f_{11} , f_{12} , and c_{11} are the feedback coefficients. Because the forward time delay, $T_R(t)$, causes $u_d(t) \neq u(t)$, we use $x_s(t)$, $\dot{x}_s(t)$, and $f_e(t)$ to adjust $u_d(t)$ as follows:

$$u_d(t) = f_{11}x_m(t - T_R(t)) + f_{12}\dot{x}_m(t - T_R(t)) + c_{11}f_h(t - T_R(t)) + f_{13}x_s(t) + f_{14}\dot{x}_s(t) + c_{12}f_e(t), \quad (2.8)$$

where f_{13} , f_{14} , and c_{12} are also the feedback coefficients.

Similarly, the slave transmitted signal, $u_s(t)$, should include force, position, and velocity:

$$u_s(t) = f_{23}x_s(t) + f_{24}\dot{x}_s(t) + c_{22}f_e(t), \quad (2.9)$$

where f_{23} , f_{24} , and c_{22} are the feedback coefficients. And since $u_{dm}(t) \neq u_s(t)$ is caused by the backward time delay, $T_L(t)$, we use $x_m(t - T(t))$, $\dot{x}_m(t - T(t))$, and $f_h(t - T(t))$ to adjust $u_{dm}(t)$ as follows:

$$\begin{aligned} u_{dm}(t) = & f_{23}x_s(t - T_L(t)) + f_{24}\dot{x}_s(t - T_L(t)) + c_{22}f_e(t - T_L(t)) \\ & + f_{21}x_m(t - T(t)) + f_{22}\dot{x}_m(t) + c_{21}f_h(t - T(t)), \end{aligned} \quad (2.10)$$

where $T(t) = T_R(t) + T_L(t)$ is the total of time delay and f_{21} , f_{22} , and c_{21} are the feedback coefficients. In this equation, $u_{dm}(t)$ can respond the control effect of $u(t - T(t))$. As a result, if we use the predicted value of $u_{dm}(t + T(t))$ as the feedback value from the slave, then the operator can feel that the time delay does not exist since the time delay on the transparency has been eliminated.

Predicted value of $u_{dm}(t + T(t))$ is labeled as $\hat{u}_{dm}(t)$ and

$$\begin{aligned} \hat{u}_{dm}(t + T(t)) = & f_{21}x_m(t) + f_{22}\dot{x}_m(t) + c_{21}f_h(t) \\ & + f_{23}\hat{x}_s(t + T_R(t)) + f_{24}\hat{\dot{x}}_m(t + T_R(t)) + c_{22}\hat{f}_e(t + T_R(t)), \end{aligned} \quad (2.11)$$

where $\hat{x}_s(t + T_R(t))$, $\hat{\dot{x}}_m(t + T_R(t))$, and $\hat{f}_e(t + T_R(t))$ are the predicted values of $x_s(t + T_R(t))$, $\dot{x}_m(t + T_R(t))$, and $f_e(t + T_R(t))$.

According to the environment model, $\hat{f}_e(t + T_R(t))$ can be estimated by the following equation:

$$\hat{f}_e(t + T_R(t)) = m_e\ddot{\hat{x}}_s(t + T_R(t)) + b_e\dot{\hat{x}}_s(t + T_R(t)) + k_e\hat{x}_s(t + T_R(t)). \quad (2.12)$$

Then, the predicted values of $\hat{x}_s(t + T_R(t))$ and $\hat{\dot{x}}_s(t + T_R(t))$ can be achieved through the time forward observer design in the next section.

3. Observer Design

Teleoperation observer is used to estimate the system parameters for the time delay compensation. The system can only achieve a high level of transparency with a good observer based on the predicted system dynamics. In order to predict $x_s(t + T_R(t))$ and $\dot{x}_s(t + T_R(t))$, (2.8) is substituted into (2.2):

$$\begin{aligned} & f_{11}x_m(t - T_R(t)) + f_{12}\dot{x}_m(t - T_R(t)) + c_{11}f_n(t - T_R(t)) \\ & + f_{13}x_s(t) + f_{14}\dot{x}_m(t) + c_{12}f_e(t) - f_e(t) \\ & = m_s\ddot{x}_s(t) + b_s\dot{x}_s(t) + k_sx_s(t). \end{aligned} \quad (3.1)$$

We define

$$\bar{u}_d(t) = f_{11}x_m(t - T_R(t)) + f_{12}\dot{x}_m(t - T_R(t)) + c_{11}f_h(t - T_R(t)). \quad (3.2)$$

Equation (3.1) becomes

$$\bar{u}_d(t) = m_s \ddot{x}_s(t) + (b_s - f_{14}) \dot{x}_s(t) + (k_s - f_{13}) x_s(t) + (1 - c_{12}) f_e(t). \quad (3.3)$$

Substituting (2.3) into (3.3),

$$\begin{aligned} \bar{u}_d(t) &= (m_s + (1 - c_{12})m_e) \ddot{x}_s(t) \\ &\quad + ((b_s - f_{14}) + (1 - c_{12})b_e) \dot{x}_s(t) \\ &\quad + ((k_s - f_{13}) + (1 - c_{12})k_e) x_s(t). \end{aligned} \quad (3.4)$$

Converting (3.4) into state-space form, we have

$$\begin{aligned} \dot{\bar{x}}_s(t) &= A_s \bar{x}_s(t) + B_s \bar{u}_d(t), \\ \bar{y}(t) &= C_s \bar{x}_s(t), \end{aligned} \quad (3.5)$$

where

$$\begin{aligned} \bar{x}_s(t) &= \begin{bmatrix} x_s(t) \\ \dot{x}_s(t) \end{bmatrix}, \quad C_s = [1 \ 0], \quad B_s = \begin{bmatrix} 0 \\ 1/m_s(1 - c_{12})m_e \end{bmatrix}, \\ A_s &= \begin{bmatrix} 0 & 1 \\ -\frac{(k_s - f_{13}) + (1 - c_{12})k_e}{m_s + (1 - c_{12})m_e} & -\frac{(b_s - f_{14}) + (1 - c_{12})b_e}{m_s + (1 - c_{12})m_e} \end{bmatrix}. \end{aligned} \quad (3.6)$$

From (3.5), in order to predict $u_{dm}(t + T(t))$, we have to prognosticate $x_s(t + T_R(t))$ and $\dot{x}_s(t + T_R(t))$ by forwarding into the future with $T_R(t)$ units:

$$\begin{aligned} \dot{\bar{x}}_s(t + T_R(t)) &= (1 + \dot{T}_R(t)) A_s \bar{x}_s(t + T_R(t)) + (1 + \dot{T}_R(t)) B_s \bar{u}_d(t + T_R(t)), \\ \bar{y}(t + T_R(t)) &= C_s \bar{x}_s(t + T_R(t)). \end{aligned} \quad (3.7)$$

However, it is difficult to estimate $\dot{T}_R(t)$. According to the characteristic of the Internet, we can model $T_R(t)$ as uncertain parameters, and (3.7) becomes

$$\begin{aligned} \dot{\bar{x}}_s(t + T_R(t)) &= (A_s + \Delta A_s) \bar{x}_s(t + T_R(t)) + (B_s + \Delta B_s) \bar{u}_d(t + T_R(t)), \\ \bar{y}(t + T_R(t)) &= C_s \bar{x}_s(t + T_R(t)), \end{aligned} \quad (3.8)$$

where $\Delta t = \dot{T}_R(t)$ and ΔA_s and ΔB_s are modeled as uncertain parameters, $\Delta A_s = \Delta t A_s$ and $\Delta B_s = \Delta t B_s$. In (3.8), when the time delay is constant, $\dot{T}_R(t) = 0$, these uncertain parameters do not exist.

Value of $\bar{x}_s(t + T_R(t))$ can be also calculated directly by the current master dynamics $x_m(t)$, $\dot{x}_m(t)$, and $f_h(t)$ via the following observer:

$$\begin{aligned}\dot{z}(t) &= A_s z(t) + B_s (f_{11} \bar{x}_m(t) + c_{11} f_h(t)) + L(\bar{y}(t + T_R(t)) - y_s(t)), \\ y_s(t) &= C_s z(t),\end{aligned}\quad (3.9)$$

where L is the observer gain, $\bar{x}_m(t) = \begin{bmatrix} x_m(t) \\ \dot{x}_m(t) \end{bmatrix}$, and $z(t) = \begin{bmatrix} \hat{x}_s(t) \\ \hat{\dot{x}}_s(t) \end{bmatrix}$.

Since the master output, $\bar{y}(t + T_R(t))$, cannot be measured, we can use the available adjustment of $t - T_L(t)$ as follows:

$$\begin{aligned}\dot{z}(t) &= A_s z(t) + B_s (f_{11} \bar{x}_m(t) + c_{11} f_h(t)) + L(\bar{y}(t - T_L(t)) - y_s(t - T_R(t) - T_L(t))), \\ y_s(t) &= C_s z(t).\end{aligned}\quad (3.10)$$

Let the observing error $e(t) = \bar{x}_s(t + T_R(t) - z(t))$, then

$$\dot{e}(t) = A_s e(t) + \Delta A_s x_s(t + T_R(t)) - L C_s e(t - T_R(t) - T_L(t)) + \Delta B_s (f_{11} \bar{x}_m(t) + c_{11} f_h(t)) \quad (3.11)$$

RBF will on line calculate the smallest $e_m(t)$, and the m th environment model which fits the best to the current environmental dynamics is selected for the system controller. Conditions for a stabilized and transparent controller are developed in the next section.

4. Controller Design

In this part, the controller design with guaranteed conditions for the system transparency and stability is established. The time forward state calculation for the slave state at $(t + T_R(t))$ has been performed in the previous section. Using $\hat{u}_{dm}(t + T(t))$ in (2.11) to take place of $u_{dm}(t)$ in (2.1), we have:

$$\begin{aligned}f_h(t) &- \left(f_{21} x_m(t) + f_{22} \dot{x}_m(t) + f_{23} \hat{x}_s(t + T_R(t)) + f_{24} \dot{\hat{x}}_s(t + T_R(t)) + c_{21} f_h(t) + c_{22} \hat{f}_e(t + T_R(t)) \right) \\ &= m_m \ddot{x}_m(t) + b_m \dot{x}_m(t) + k_m x_m(t).\end{aligned}\quad (4.1)$$

Rearranging (4.1) yields

$$\begin{aligned}m_m \ddot{x}_m(t) &+ (b_m + f_{22}) \dot{x}_m(t) + (k_m + f_{21}) x_m(t) \\ &= - \left(f_{23} \hat{x}_s(t + T_R(t)) + f_{24} \dot{\hat{x}}_s(t + T_R(t)) + c_{22} \hat{f}_e(t + T_R(t)) \right).\end{aligned}\quad (4.2)$$

Substituting (2.12) into (4.2) and modifying, we have

$$\begin{aligned} m_m \ddot{x}_m(t) + (b_m + f_{22}) \dot{x}_m(t) + (k_m + f_{21}) x_m(t) \\ = -((f_{23} + c_{22}k_e) \hat{x}_s(t + T_R(t)) + (f_{24} + c_{22}b_e) \dot{\hat{x}}_s(t + T_R(t)) + c_{22}m_e \ddot{\hat{x}}_s(t + T_R(t))) \\ + (1 - c_{21}) f_h(t). \end{aligned} \quad (4.3)$$

Using $z(t)$ in (3.9) replacing $\hat{x}_s(t)$ in (4.3), we have

$$\ddot{x}_m(t) + \frac{(b_m + f_{22})}{m_m} \dot{x}_m(t) + \frac{(k_m + f_{21})}{m_m} x_m(t) = \frac{(1 - c_{21})}{m_m} f_h(t) - (A_e z(t) + B_e \dot{z}(t)), \quad (4.4)$$

where

$$A_e = \left[\frac{(f_{23} + c_{22}k_e)}{m_m} \quad \frac{(f_{24} + c_{22}b_e)}{m_m} \right], \quad B_e = \left[0 \quad \frac{c_{22}m_e}{m_m} \right]. \quad (4.5)$$

Substituting (3.9) into (4.4) and altering, we have

$$\begin{aligned} \ddot{x}_m(t) + \frac{(b_m + f_{22})}{m_m} \dot{x}_m(t) + \frac{(k_m + f_{21})}{m_m} x_m(t) \\ = -(A_e + B_e A_s) z(t) + B_e B_s (f_{11} \bar{x}_m(t) + c_{11} f_h(t)) + B_e L C_s e^{(t - t(T))} + \frac{(1 - c_{21})}{m_m} f_h(t) \end{aligned} \quad (4.6)$$

or

$$\begin{aligned} \ddot{x}_m(t) + \left(\frac{(b_m + f_{22})}{m_m} + B_e B_s f_{12} \right) \dot{x}_m(t) + \left(\frac{(k_m + f_{21})}{m_m} + B_e B_s f_{11} \right) x_m(t) \\ = \left(\frac{(1 - c_{21})}{m_m} + B_e B_s c_{11} \right) f_h(t) - ((A_e + B_e A_s) z(t) + B_e L C_s e^{(t - T(t))}). \end{aligned} \quad (4.7)$$

Converting (4.7) into state-space form, we have

$$\begin{aligned} \dot{\bar{x}}_m(t) &= A_m \bar{x}_m(t) + B_m f_h(t) - (A_z(\bar{x}_s(t + T_R(t)) - e(t)) + B_z e^{(t - T(t))}), \\ y_m(t) &= C_m \bar{x}_m(t), \end{aligned} \quad (4.8)$$

where

$$A_m = \begin{bmatrix} 0 & 1 \\ -\left(\frac{k_m + f_{21}}{m_m} + B_e B_s f_{11}\right) & -\left(\frac{b_m + f_{22}}{m_m} + B_e B_s f_{12}\right) \end{bmatrix}, \quad C_m = [1 \ 0], \quad (4.9)$$

$$B_m = \begin{bmatrix} 0 \\ \frac{1 - c_{11}}{m_m} + B_e B_s c_{11} \end{bmatrix}, \quad A_z = \begin{bmatrix} 0 \\ A_e + B_e A_s \end{bmatrix}, \quad B_z = \begin{bmatrix} 0 \\ B_e LC_s \end{bmatrix}. \quad (4.10)$$

From (3.8), (3.11), and (4.8), the model of total system is established as

$$\begin{aligned} \dot{x}(t) &= Ax(t) + A_t x(t - T(t)) + B f_h(t), \\ y(t) &= Cx(t), \end{aligned} \quad (4.11)$$

where

$$\begin{aligned} x(t) &= \begin{bmatrix} \bar{x}_m(t) \\ \bar{x}_s(t + T_R(t)) \\ e(t) \end{bmatrix}, \quad A = \begin{bmatrix} A_m & -A_z & A_z \\ (B_s + \Delta B_s) f_{11} & A_s + \Delta A_s & 0 \\ \Delta B_s f_{11} & \Delta A_s & A_s \end{bmatrix}, \quad C = \begin{bmatrix} C_m & 0 & 0 \\ 0 & C_s & 0 \\ 0 & 0 & 0 \end{bmatrix}, \\ B &= \begin{bmatrix} B_m \\ (B_s + \Delta B_s) c_{11} \\ \Delta B_s c_{11} \end{bmatrix}, \quad A_t = \begin{bmatrix} 0 & 0 & -B_z \\ 0 & 0 & 0 \\ 0 & 0 & -LC_s \end{bmatrix}. \end{aligned} \quad (4.12)$$

The model of total system in (4.11) is now subject to conditions for the system transparency as referred to by Lawrence [4] that a teleoperation system achieves stability and ideal transparency if the following relation is maintained:

$$\frac{F_e(s)}{X_s(s)} = \frac{F_h(s)}{X_m(s)}, \quad (4.13)$$

where $F_e(s)$, $X_s(s)$, $F_h(s)$, and $X_m(s)$ are the Laplace transform of $f_e(t)$, $x_s(t)$, $f_h(t)$, and $x_m(t)$, respectively.

Substituting (2.2), (2.3), (2.8), and (2.10) into (4.13), following conditions for the system transparency yield:

$$\begin{aligned}
& ((1 - c_{21})(m_s + (1 - c_{12})m_e) - c_{11}c_{22}m_e)m_e = (m_s + (1 - c_{12})m_e)m_m, \\
& ((1 - c_{21})(m_s + (1 - c_{12})m_e) - c_{11}c_{22}m_e)b_e \\
& \quad + (1 - c_{12})(b_s - f_{14} + (1 - c_{12})b_e - c_{11}(f_{24} + c_{22}b_e))m_e \\
& \quad = (b_s - f_{14} + (1 - c_{12})b_e)m_m + (m_s + (1 - c_{12})m_e)(b_m + f_{22}) + c_{22}m_e f_{12}, \\
& ((1 - c_{21})(m_s + (1 - c_{12})m_e) - c_{11}c_{22}m_e)k_e \\
& \quad + ((1 - c_{12})(b_s - f_{14} + (1 - c_{12})b_e - c_{11}(f_{24} + c_{22}b_e))b_e \\
& \quad \quad + (1 - c_{21})(k_s - f_{13} + (1 - c_{12})k_e) - c_{11}(f_{23} + c_{22}k_e))m_e \\
& \quad = (k_s - f_{13} + (1 - c_{12})k_e)m_m + (b_s - f_{14} + (1 - c_{12})b_e)(b_m + f_{22}) \tag{4.14} \\
& \quad \quad + (m_s + (1 - c_{12})m_e)(k_m + f_{21}) + c_{22}m_e f_{11} + (f_{24} + c_{22}b_e)f_{12} \\
& ((1 - c_{21})(b_s - f_{14} + (1 - c_{12})b_e) - c_{11}(f_{24} + c_{22}b_e))k_e \\
& \quad + (1 - c_{21})(k_s - f_{13} + (1 - c_{12})k_e) - c_{11}(f_{23} + c_{22}k_e)b_e \\
& \quad = (k_s - f_{13} + (1 - c_{12})k_e)(b_m + f_{22}) + (b_s - f_{14} + (1 - c_{12})b_e)(b_m + f_{21}) \\
& \quad \quad + (f_{24} + c_{22}b_e)f_{11} + (f_{23} + c_{22}k_e)f_{12}, \\
& ((1 - c_{21})(k_s - f_{13} + (1 - c_{12})k_e) - c_{11}(f_{23} + c_{22}b_e))k_e \\
& \quad = (k_s - f_{13} + (1 - c_{12})k_e)(k_m + f_{21}) + (f_{23} + c_{22}k_e)f_{11}.
\end{aligned}$$

Consequently, if (4.14) is feasible, the system will achieve the stability and ideal transparency. Simulations for this controller are examined in the next section.

5. Simulation Results

Simulation of this proposed model is developed with Matlab/Simulink for time-variant delays and environment uncertainties. The controller is also tested for the ability to reject disturbances while maintaining its closed-loop stability.

In the simulation, the parameters of the master and slave manipulator are selected as $m_m = 1.5$ kg, $b_m = 0.45$ Ns/m, $k_m = 1$ N/m, $m_s = 1.5$ kg, $b_s = 0.45$ Ns/m, and $k_s = 1$ N/m. It is assumed that the environment uncertainties consist of three models M_1 , M_2 , and M_3 activated randomly.

The parameters of environment model M_1 are selected as $m_{e1} = 1.1$ kg, $b_{e1} = 0.6$ Ns/m, and $k_{e1} = 0.6$ N/m. The initial controller parameters are chosen as $c_{11} = 30$, $f_{11} = 2$, $f_{12} = 1$, $f_{21} = 1456$, and $f_{22} = 987$. To assure the system transparency, other controller parameters are calculated as solutions of (4.14) as $c_{12} = -27.636$, $c_{21} = -29$, $c_{22} = 28.636$, $f_{13} = -1.8182$, $f_{14} = -1.3682$, $f_{23} = -1456.2$, and $f_{24} = -986.63$.

Similarly, the parameters of environment model M_2 are selected as $m_{e2} = 1.0$ kg, $b_{e2} = 0.4$ Ns/m, and $k_{e2} = 0.8$ N/m. Then, other initial controller parameters are chosen as $c_{11} = 20$,

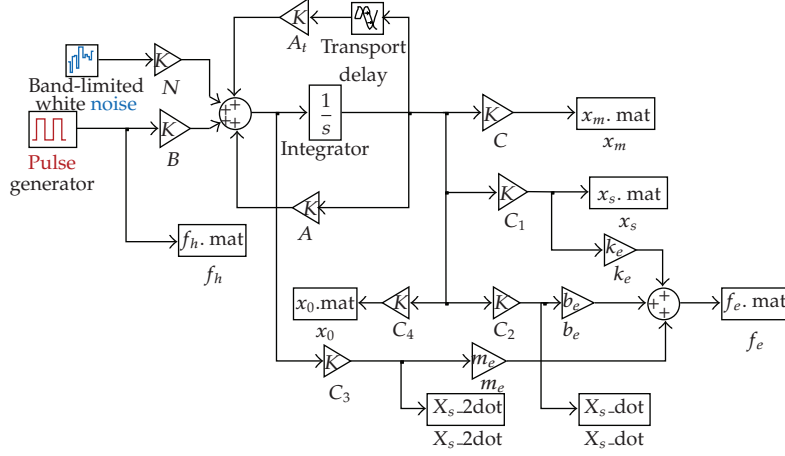


Figure 5: Matlab Simulink diagram.

$f_{11} = 2$, $f_{12} = 1$, $f_{21} = 1500$, and $f_{22} = 1200$. For transparency conditions, the remaining controller parameters are calculated as $c_{12} = -17.5$, $c_{21} = -19$, $c_{22} = 18.5$, $f_{13} = -2.2$, $f_{14} = -1.15$, $f_{23} = -1499.8$, and $f_{24} = -1199.8$.

The parameters of environment model M_3 are selected as $m_{e3} = 1.5$ kg, $b_{e3} = 0.7$ Ns/m, and $k_{e3} = 0.5$ N/m. The initial controller parameters in this case are chosen as $c_{11} = 30$, $f_{11} = 2$, $f_{12} = 1$, $f_{21} = 1497$, and $f_{22} = 1356$. Conditions for the system transparency lead to other controller parameters as $c_{12} = -28$, $c_{21} = -29$, $c_{22} = 29$, $f_{13} = -1.5$, $f_{14} = -1.25$, $f_{23} = -1497.5$, and $f_{24} = -1355.8$.

The time-variant delays in the communication channel are randomly selected with $0 < T_R(t) \leq 5$ s and $0 < T_L(t) \leq 5$ s. The three environmental uncertainties, M_1 , M_2 , and M_3 are also randomly activated, and the RBF network is used to select the best fitted model. The maximum allowable bound of time delay, $T_{\text{Max_DeLay}}$, for guaranteeing stability of the system therefore is the sum of the maximum of forward time delay, $T_{\text{Max_R}}(t)$, and the maximum of backward time delay, $T_{\text{Max_L}}(t)$, $T_{\text{Max_DeLay}} \leq T_{\text{Max_R}}(t) + T_{\text{Max_L}}(t) = 10$ s.

The input human force, f_h , with pulse generator activates the movement of the master device, x_m . Three environment models, M_1 , M_2 , and M_3 , are activated at time from timeline from 0–30 s, 31–60 s, and 61–90 s, respectively. RBF identifies the environmental parameters and activates the suitable adaptive controllers. A white noise is also injected to the system to test the ability of the system to maintain its stability as shown in Figure 5.

Results of the simulation for the time-variant delays and the environmental uncertainties are shown in Figure 6. The subplots indicate the forces and movements of the master and the slave. The adaptive predictive controller is accurate, and the system is stable and in good performance since the slave profiles tracking well to the master amid the time-variant delays and the environment uncertainties.

Lastly, the model is tested for the ability to maintain its closed-loop stability with noise disturbances. Simulation results for the time-variant delays and the environmental uncertainties with noises are shown in Figure 7.

Simulation results show that the system is stable under the white-noise disturbances. The outputs can track the input properly without steady-state error. The controller is robust to the disturbances.

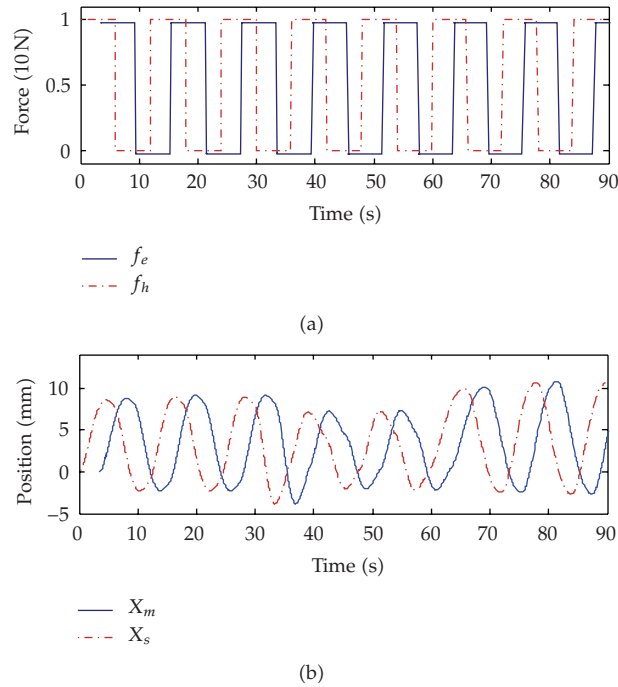


Figure 6: Position of master and slave with time-variant delays and environmental uncertainties.

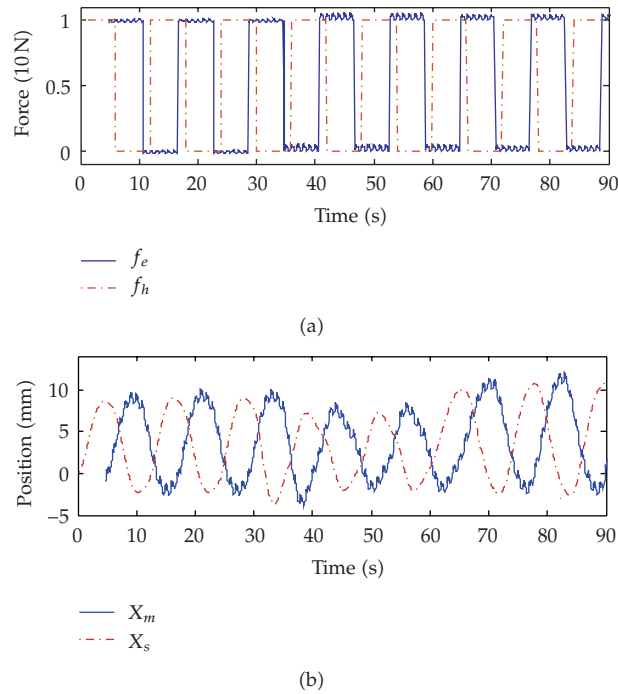


Figure 7: Position of master and slave with time-variant delays and noises.

6. Conclusion

This paper presents a novel theoretical framework to design a teleoperation system dealing with time-variant delays and environmental uncertainties. Using predictive strategies and RBF network, the stability and transparency of the system are guaranteed amid the noise disturbance. The RBF neural network is trained off line using a set of environmental models and selects the best fitted model in the current environment dynamics. Issue of communication uncertain delays in teleoperation is also addressed. A neural network-based multiple-model adaptive controller is proposed to design the time forward state observer. Simulations show that the system is stable and in good performance. However, the system becomes unstable if conditions for the stability and transparency are not feasible. Further analysis is needed for the effectiveness with respect to the achievable performance and reliability of this design.

Acknowledgment

The authors would like to thank the comments provided by the anonymous reviewers and editor, which help the authors improve this paper significantly. The authors have taken into consideration all comments of the reviewers in the final version of the paper. This work was supported by Universiti Teknologi PETRONAS (UTP) and funded by Project FRGS 2/2010/TK/UTP/02/28 from Ministry of Higher Education, Malaysia (MOHE).

References

- [1] J. Kikuchi, K. Takeo, and K. Kosuge, "Teleoperation system via computer network for dynamic environment," in *Proceedings of the IEEE International Conference on Robotics and Automation*, pp. 3534–3539, Leuven, Belgium, May 1998.
- [2] W. Zhu and S. E. Salcudean, "Teleoperation with adaptive motion/force control," in *Proceedings of the IEEE International Conference on Robotics and Automation (ICRA '99)*, pp. 231–237, Detroit, Mich, USA, May 1999.
- [3] M. Boukhnifer and A. Ferreira, "Stability and transparency for scaled teleoperation system," in *Proceedings of the IEEE/RSJ International Conference on Intelligent Robots and Systems*, pp. 4217–4222, Beijing, China, 2006.
- [4] D. A. Lawrence, "Stability and transparency in bilateral teleoperation," *IEEE Transactions on Robotics and Automation*, vol. 9, no. 5, pp. 624–637, 1993.
- [5] E. Slawiński and V. Mut, "Transparency in time for teleoperation systems," in *Proceedings of the IEEE International Conference on Robotics and Automation (ICRA '08)*, pp. 200–205, Pasadena, Calif, USA, May 2008.
- [6] Q. Chen, J. Quan, and J. Xia, "Neural network based multiple model adaptive predictive control for teleoperation system," in *Proceeding of the 4th International Symposium on Neural Networks: Advances in Neural Networks*, vol. 4491, pp. 64–69, Nanjing, China, 2007.
- [7] A. C. Smith and K. Hashtrudi-Zaad, "Adaptive teleoperation using neural network-based predictive control," in *Proceedings of the IEEE Conference on Control Applications*, pp. 1269–1274, Toronto, Canada, 2005.
- [8] A. Suebsomran and M. Parnichkun, "Disturbance observer-based hybrid control of displacement and force in a medical tele-analyzer," *International Journal of Control, Automation and Systems*, vol. 3, no. 1, pp. 70–78, 2005.
- [9] K. Hashtrudi-Zaad and S. E. Salcudean, "Transparency in time-delayed systems and the effect of local force feedback for transparent teleoperation," *IEEE Transactions on Robotics and Automation*, vol. 18, no. 1, pp. 108–114, 2002.
- [10] V. T. Minh, N. Afzulpurkar, and W. M. W. Muhamad, "Fault detection and control of process systems," *Mathematical Problems in Engineering*, vol. 2007, Article ID 80321, 20 pages, 2007.

- [11] O. M. Kwon and J. H. Park, "Exponential stability for uncertain cellular neural networks with discrete and distributed time-varying delays," *Applied Mathematics and Computation*, vol. 203, no. 2, pp. 813–823, 2008.
- [12] J. H. Park and O. M. Kwon, "Delay-dependent stability criterion for bidirectional associative memory neural networks with interval time-varying delays," *Modern Physics Letters B*, vol. 23, no. 1, pp. 35–46, 2009.